Vitrification and gelation in sticky spheres

C. Patrick Royall, Stephen R. Williams, and Hajime Tanaka
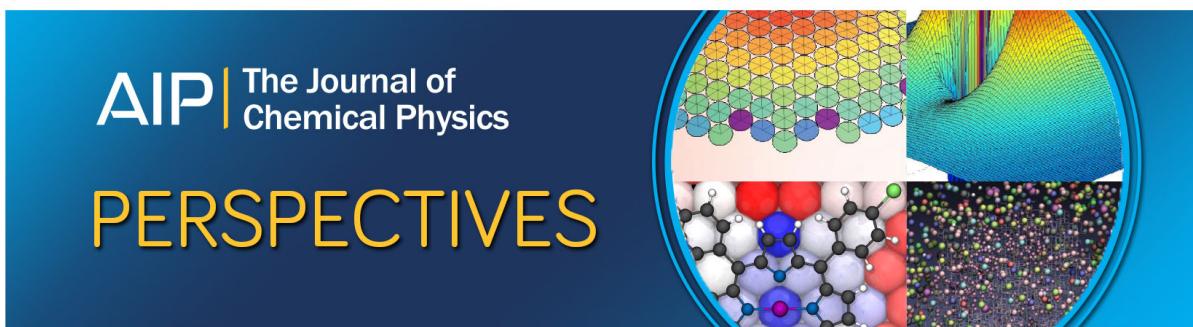
Vitrification and gelation in sticky spheres

C. Patrick Royall,[1,2,3,a)] Stephen R. Williams,[4] and Hajime Tanaka[5,b)]

[1]*HH Wills Physics Laboratory, Tyndall Avenue, Bristol BS8 1TL, United Kingdom*
[2]*School of Chemistry, University of Bristol, Cantock Close, Bristol BS8 1TS, United Kingdom*
[3]*Centre for Nanoscience and Quantum Information, Tyndall Avenue, Bristol BS8 1FD, United Kingdom*
[4]*Research School of Chemistry, Australian National University, Canberra, ACT 0200, Australia*
[5]*Department of Fundamental Engineering, Institute of Industrial Science, University of Tokyo,*
4-6-1 Komaba, Meguro-ku, Tokyo 153-8505, Japan

Glasses and gels are the two dynamically arrested, disordered states of matter. Despite their importance, their similarities and differences remain elusive, especially at high density, where until now it has been impossible to distinguish them. We identify dynamical and structural signatures which distinguish the gel and glass transitions in a colloidal model system of hard and "sticky" spheres. It has been suggested that "spinodal" gelation is initiated by gas-liquid viscoelastic phase separation to a bicontinuous network and the resulting densification leads to vitrification of the colloid-rich phase, but whether this phase has sufficient density for arrest is unclear [M. A. Miller and D. Frenkel, Phys. Rev. Lett. **90**, 135702 (2003) and P. J. Lu *et al.*, Nature **435**, 499–504 (2008)]. Moreover alternative mechanisms for arrest involving percolation have been proposed [A. P. R. Eberle *et al.*, Phys. Rev. Lett. **106**, 105704 (2011)]. Here we resolve these outstanding questions, beginning by determining the phase diagram. This, along with demonstrating that percolation plays no role in controlling the dynamics of our system, enables us to confirm spinodal decomposition as the mechanism for gelation. We are then able to show that gels can be formed even at much higher densities than previously supposed, at least to a volume fraction of $\phi = 0.59$. Far from being networks, these gels apparently resemble glasses but are still clearly distinguished by the "discontinuous" nature of the transition and the resulting rapid solidification, which leads to the formation of *inhomogeneous* (with small voids) and *far-from-equilibrium local structures*. This is markedly different from the glass transition, whose continuous nature leads to the formation of *homogeneous and locally equilibrated structures*. We further reveal that the onset of the attractive glass transition in the form of a supercooled liquid is in fact interrupted by gelation. Our findings provide a general thermodynamic, dynamic, and structural basis upon which we can distinguish gelation from vitrification. *Published by AIP Publishing.*
https://doi.org/10.1063/1.5000263

I. INTRODUCTION

Dynamical arrest remains one of the principal unsolved challenges in condensed matter.[1] In everyday soft materials, arrest takes two forms: vitrification, the process by which a fluid becomes a glass,[1] and gelation, a transition to the gel state.[2,3] A glass is known to have spatially homogeneous density on length scales larger than a few particle diameters.[4] On the other hand, gelation corresponds to arrest via a number of routes:[3] Some gels are thermodynamically indistinguishable from glasses,[5–7] while in many materials, such as colloids,[2,3,8–11] proteins,[12–14] and some polymers,[15] it has been suggested that gelation is induced by spinodal decomposition to two phases whose dynamics are very different[10,16] and the resulting vitrification of the slower phase then drives arrest. However other mechanisms have been proposed,[17,18] and discrepancies in the literature[11,19] cast some doubt over

spinodal decomposition as the mechanism. Here we consider the mechanism of gelation and its relationship to vitrification by using the "sticky sphere" system as a model.[2,8–11]

An archetypal colloidal gel has a sparse percolated network structure at low overall colloid concentration. However, with an increase in concentration, the network structure becomes thicker and the material more homogeneous in density, which makes the distinction between gels and glasses increasingly obscure. The comparison between these non-ergodic states has so far been dominated by considerations of glasses and gels with very different densities.[2,3] For elucidating the fundamental difference between the glass transition and gelation, however, the critical comparison should be made for a gel and a glass at *similar* density. Since glasses are formed at high density, this comparison should be made at high density, but there both glasses and gels form similar disordered non-ergodic structures, which are rather homogeneous beyond the particle scale. This makes the comparison very challenging. While it is possible to make a dynamical distinction between glasses and gels using rheology[20,21] or simulation,[22,23] these measures suggest a crossover in

a)Electronic mail: chcpr@bristol.ac.uk
b)Electronic mail: tanaka@iis.u-tokyo.ac.jp

dynamical behavior, rather than a sharp transition between arrested and non-arrested states. This is due to the emphasis on the interplay of caging (glass) and bonding (gel) behavior. Since the onset of vitrification is continuous,[1] the interplay between these effects is also continuous. We are thus left with a rather fuzzy notion of where the gel ends and the glass begins.

Here we aim for a clear, well-defined distinction between glasses and gels. To make progress in this direction, we consider thermodynamic properties. First we consider the mechanism of gelation. This enables us to identify a clear transition between gelation and vitrification which reveals fundamental differences between the two types of ergodic-nonergodic transitions. We can then address questions such as what physical factors allow us to distinguish these two non-ergodic states and whether the transition between them is continuous or discontinuous.

In the absence of attraction, colloidal "hard" spheres undergo a glass transition upon increasing volume fraction.[2,24] The addition of polymers leads to an effective attraction between the colloids due to polymer depletion whose range and strength are set by the polymer size and concentration, respectively. The strength of this polymer-mediated colloid-colloid interaction sets an effective temperature. Upon increasing the polymer concentration, the effective temperature is reduced and systems with short-ranged (sticky) attractions undergo gelation at moderate colloid volume fractions.[2,3,25,26] At high volume fraction, the hard sphere glass melts upon the introduction of attractions and the resulting (ergodic) fluid subsequently undergoes re-entrant dynamical arrest upon increasing the attraction strength.[2,27–32] A key question we pursue here is to ascertain the nature of this re-entrant dynamical arrest.

Important insights have been gained by exploiting the fact that demixing can be suppressed by the addition of a long-ranged repulsion.[18,33] However full suppression of demixing is not always realized,[34] and in the absence of an equilibrium phase diagram, behavior such as microphase separation and long-lived metastable states[35,36] can lead to phenomena hard to distinguish from the case without long-ranged repulsion that we consider here. Our standpoint is that at the present time, we are left with no clear picture of exactly how to distinguish a glass and a gel at high density.

We take the following approach to distinguish gels and glasses. A supercooled liquid becomes a glass when the structural relaxation time exceeds the experimental time scale. At higher densities (or lower temperatures), lack of equilibration makes it hard to determine the existence or otherwise any thermodynamic signature of the glass transition.[1] In the case of gels, it has been suggested that gelation is related to spinodal liquid-gas phase separation involving inhomogenization of the colloid density.[8–11,37,38] However the literature appears somewhat divided on this matter. First, in simulations of the Baxter model of sticky spheres, the volume fraction of the colloid-rich phase is found to be $\lesssim 0.5$,[19] differing from that deduced in experiments.[11] We expect that a volume fraction around 0.5 is insufficient for dynamical arrest. This suggests that some other mechanism should be at play, i.e., spinodal demixing by itself is not enough to form an arrested network. Such a

mechanism has been proposed in the form of percolation of the colloids, which occurs at much lower colloid volume fraction and attraction strength.[17] In short, different interpretations of the equilibrium phase diagram have been proposed and multiple mechanisms have been presented to explain gelation in sticky spheres.

Here we address these issues concerning the nature of gelation and distinguishing glasses and gels with a combination of experiments and computer simulations. By obtaining the phase diagram and percolation line, we confirm spinodal decomposition as the mechanism for gelation in sticky spheres. This enables us to distinguish gelation and vitrification. We show that gelation is quasi-discontinuous while the approach to vitrification is continuous as a function of (effective) temperature or density.

Following a discussion of our methodology which combines particle resolved studies[39] and event-driven molecular dynamics simulations[40] in Sec. II, our results are laid out in Sec. III: by confirming spinodal decomposition as the gelation mechanism, we can now provide clear physical measures that enable discrimination between gels and glasses unlike the dynamical approach considered previously.[20–22] This distinction is clearly shown in the relaxation time (Sec. III B), topological characteristics, local structural measures (Sec. III E), and (osmotic) pressure (Sec. III D). The former three show a quasi-discontinuous jump upon gelation and a continuous change upon the approach to vitrification, while the latter turns negative at gelation but rises approaching vitrification for hard spheres. This framework enables us to distinguish gelation and vitrification unambiguously. Remarkably, we find a signature of the attractive glass predicted by mode coupling theory (MCT) but that its onset is interrupted by gelation which we discuss in Sec. III C. In Sec. III F, we use our results from gels to identify signatures in local structure which reveal that the system is far from equilibrium in the case of "hyperquenched" glasses. Finally, we consider aging in gels in Sec. III G. Having established the nature of vitrification and gelation in sticky spheres, we then discuss the generality of our results for other systems in Sec. IV.

II. MATERIALS AND METHODS

A. Experimental

We carry out confocal microscopy experiments where we track the colloids at the single-particle level. We use fluorescently labeled density and refractive index matched colloids. We used two systems, both of sterically stabilized polymethyl methacrylate colloids. The first system used particles of diameter $\sigma = 2.40$ μm with size polydispersity 4%, determined with static light scattering. The polystyrene polymer had a molecular weight of $M_w = 3.1 \times 10^7$, leading to a polymer-colloid size ratio of $q = 0.18$.[42] We used the first system for the path in the state diagram in Fig. 1 marked ($\overline{ba}$). Otherwise, we used a system with $\sigma = 3.23$ μm, as determined from the first peak of $g(r)$ from confocal microscopy data, and 6% polydispersity, determined with SEM. For the weakly polydisperse systems of interest here, the two methods of determining polydispersity give similar results.
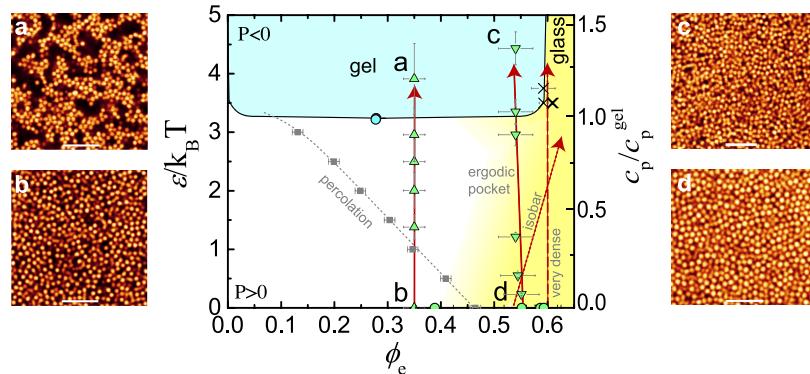
FIG. 1. Phase diagram of sticky spheres (3% square well), with mapped experimental data. ε is the well depth (inverse effective temperature), c_p/c_p^{gel} is the polymer mass fraction c_p relative to that required for gelation c_p^{gel}, and ϕ_e is the (effective) colloid volume fraction. The turquoise circle is the critical point.[41] P denotes the sign of (osmotic) pressure. Crosses indicate the volume fraction of the dense phase estimated from fully phase separated simulations. These are used to construct the liquid-gas phase separation line which delimits the gel region. Percolation is indicated as grey squares with a dashed line to guide the eye. Shaded areas indicate the onset of slow dynamics. Arrows denote different paths considered, with green symbols denoting experimental data points. $(\overline{bd})$ (circles) corresponds to the hard sphere glass transition, $(\overline{ba})$ (up triangles) corresponds to gelation at moderate ϕ_e, and $(\overline{dc})$ (down triangles) corresponds to gelation at high ϕ_e. The long dashed arrow marked "very dense" refers to a supercooled liquid-fluid-supercooled liquid-gel path at very high $\phi_e = 0.59$. The isobaric quench is shown as a dotted arrow. Confocal images of state points indicated in the phase diagram are as follows: (a) "normal gel" ($\phi_e = 0.35$, $c_p/c_p^{gel} = 1.14$); (b) "hard spheres" ($\phi_e = 0.35$); (c) high-density gel ($\phi_e = 0.54$, $c_p/c_p^{gel} = 1.43$); (d) "hard spheres" ($\phi_e = 0.58$). Bars = 20 μm.

The polymer had $M_w = 8.06 \times 10^6$ ($q = 0.079$). We assume that the degrees of freedom of the polymers can be integrated out and the system can be treated as an effective one-component colloid system. For the size ratios we consider, this is expected to be accurate.[43]

In both cases, the colloids and polymers were dispersed in a density- and refractive index-matching mixture of *cis*-decalin and cyclohexyl bromide. 4 mmol of tetrabutylammonium bromide salt was added to screen electrostatic interactions. Despite screening, the electrostatic interactions can lead to an increase in *effective* colloid volume fraction ϕ_e compared to the absolute volume fraction ϕ.[44] Here we use ϕ_e throughout. Brownian times to diffuse a radius were $\tau_B = 3.11$ s and 7.59 s for the $\sigma = 2.40$ μm and $\sigma = 3.32$ μm systems, respectively. We find gelation at $c_p^{gel} = 1.0 \pm 0.2 \times 10^{-3}$ and $c_p^{gel} = 1.29 \pm 0.08 \times 10^{-4}$ for the "gel" and "dense" paths in Fig. 1, respectively.

We chose two strategies in preparing our samples. For the path $(\overline{ba})$ in Fig. 1, we mixed each sample from stock solutions of colloids in *cis*-decalin, polymers dissolved in *cis*-decalin, and cyclohexyl bromide in which the tetrabutylammonium bromide salt was dissolved. Additional *cis*-decalin or salt solution was added to ensure density matching.

For the high-density and hard sphere samples, we used a density-matched stock solution of "hard" spheres. This was centrifuged at 35 °C; the higher temperature removed the density matching, allowing a sediment to be produced. To this was added further the *cis*-decalin solvent, the *cis*-decalin polymer solution, and a saturated solution of tetrabutylammonium bromide in cyclohexyl bromide to produce high-volume fraction samples. Chemicals were purchased from Fluka and used as received. The colloids were synthesized following Bosma *et al.*[45] and Zerrouki *et al.*[46] for the $\sigma = 2.40$ μm and $\sigma = 3.23$ μm colloids, respectively.

The samples were imaged with a Leica SP5 confocal microscope fitted with a resonant scanner. Prior to imaging,

the samples were loaded into borosilicate glass capillaries (obtained from Vitrocom, Inc.) and sealed with epoxy resin. We allowed the resin to set for 15 min prior to imaging and took data after letting the samples rest for further 15 min. Imaging was carried out with the temperature fixed at 27 °C with a temperature controlled stage and objective lens. During imaging, we saw no aging of the samples on the experimental time scale (up to three days). In another work, we have identified that initial remixing prior to arrest in gelation occurs on a time scale of less than 1 min.[47]

The observed behavior is generic to systems with short-range attraction such as those we consider.[48] The experiments are thus mapped to event-driven molecular dynamics (MD) simulations. Further details are given in Sec. II D.
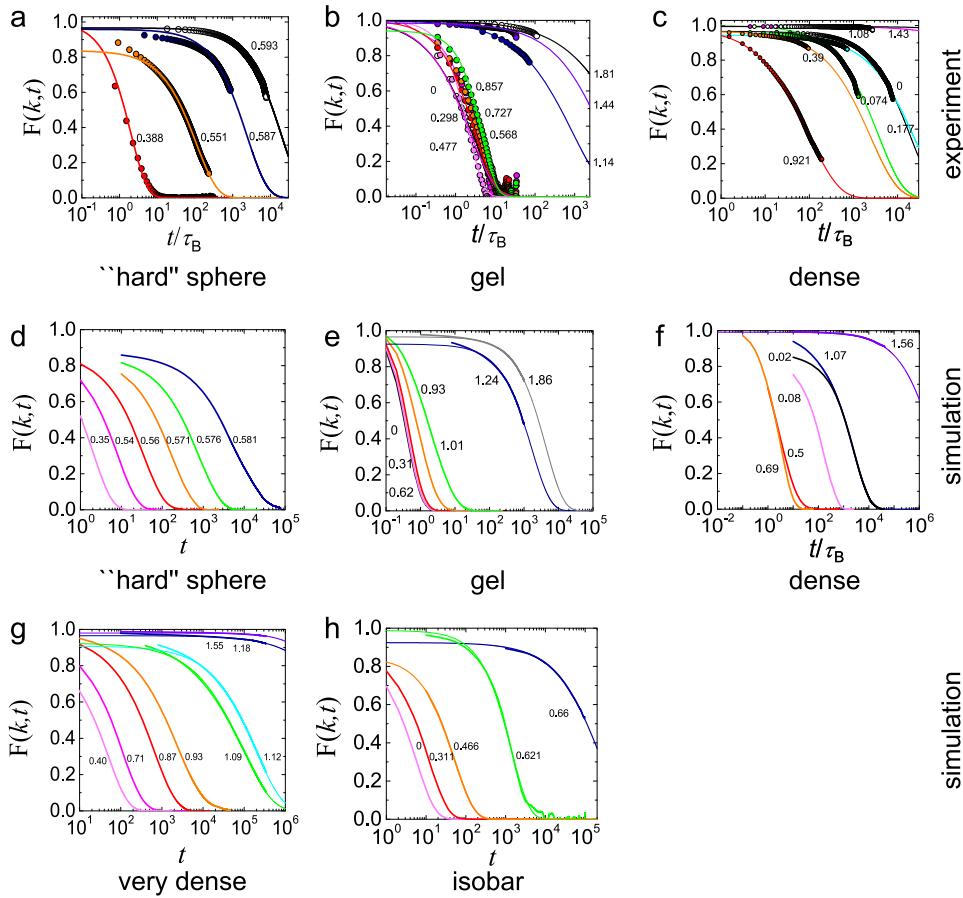
B. Computer simulation

Event-driven molecular dynamics (MD) simulations were carried out with the DynamO package.[40] While other techniques, such as Gibbs ensemble Monte Carlo, are available for the determination of a phase diagram (see Sec. III A), here the dynamics are prohibitively slow for such techniques. Newer methods, such as particle swaps, are in principle attractive; however, here we seek to mimic the experimental system, whose polydispersity of 6% lies far below that currently accessible to this method.[49] We therefore elect to use MD here.

We used an equimolar five-component mixture whose polydispersity is 8%, interacting with a square well of width 0.03σ, where σ is the particle diameter and well depth ε. The latter is proportional to polymer mass fraction c_p in the experimental system, so we express state points in volume fraction ϕ_e and ε or c_p. We selected a polydispersity of 8% for the simulations in order to suppress crystallisation, which we occasionally encountered with a lower polydispersity. Gelation accompanied by crystallization, i.e., crystal gel

formation, is observed in a rather monodisperse colloidal suspension for a shallow quench.[47,50–57] Recently it was shown[57] that it is necessary for crystal gel formation to have a relaxation of the mechanical stress built up in a transient network and the resulting reorganization of the network to a more compact network. The increase in the number of bonds after network reorganization is a necessary condition for crystallization, as more compact environments become available to accommodate the critical nucleus size, while in its absence, the network forms low-density arrested states (gels). This condition is to be met only when bonds are weak enough—that is, at low polymer concentrations. In any case, our structural analysis (see Sec. II E) is sensitive to crystallisation, and we see only trace amounts of crystalline local environments here.

We equilibrated for at least 10 τ_α and (unless otherwise indicated) sampled for at least a further 10 τ_α, where τ_α is the structural relaxation time. Simulation time was scaled to experimental data such that τ_α for $\phi_e \approx 0.38$ was matched between both, namely, $\tau_\alpha = 2.597\,\tau_B$ which is then equivalent to the MD value of 0.404 simulation time units. Under this mapping of simulation, equilibration times are at least as large as those of the experiments. Percolation is determined by requiring that more than 50% of snapshots have a cluster spanning the system in at least one Cartesian axis for a system of $N = 32\,000$ particles. For percolation, we take the bond length of 0.03σ and consider a monodisperse system. Our analysis reveals a clear percolation threshold and is relatively insensitive to the details of the size threshold we use,[58] and certainly for our

purposes here, sufficient to show that percolation and gelation are independent phenomena. We elect to use a monodisperse system here for simplicity, noting that at the fluid state points we consider, monodisperse systems are almost indistinguishable from weakly polydisperse systems.[54]

C. Dynamical analysis

We estimate the structural relaxation time τ_α from the intermediate scattering function (ISF), $F(\mathbf{k}, t) = \langle \sum_{j=1}^{N} \exp[i\mathbf{k} \cdot (\mathbf{r}(t+t') - \mathbf{r}(t'))] \rangle$, where the sum runs over all particles in the system. This we determine from coordinate data in the case of both experiments and simulations. The length scale upon which mobility is probed is set by the wavevector k which here is taken to correspond to a particle diameter ($k \sim 2\pi\sigma^{-1}$). The long-time tail of the ISF is fitted with a stretched exponential whose time constant is τ_α. The wavevector is taken close to the main peak in the static structure factor. Fits to ISFs with a stretched exponential are shown as solid lines in Figs. 2(a)–2(c) and light lines in Figs. 2(d)–2(f). For very deep quenches, the ISF does not fully relax on the experimental or simulation time scale. In the case of simulation, we run the system for 10^5 simulation time units and sample for a further 10^5 time units except in the "very dense" case (Fig. 2). There we run the system for 5×10^5 time units and sample for a further 5×10^5 time units. We find that simulations do not equilibrate in the gel region of the state diagram, except in the case of weak quenches where complete phase separation is observed.

FIG. 2. Intermediate scattering functions. (a)–(c): Intermediate scattering functions determined from experiments for the "hard" sphere $(\overline{bd})$ (a), gel $(\overline{ba})$ (b), and dense gel $(\overline{dc})$ (c) paths in Fig. 1. (d)–(h): Simulation data, for the "hard" sphere (d), gel (e), dense gel (f), very dense (g), and isobaric (h) paths. Experimental data are in units of Brownian time τ_B, and simulation data are in simulation time units. In (a) and (d), ISFs are shown at different ϕ_e, whereas in (b), (c), and (e)–(h) labels denote c_p/c_p^{gel}. All ISFs are fitted with stretched exponentials to obtain τ_α which are shown as solid lines in (a)–(c) and light lines in (d)–(h). For very deep quenches, the ISF does not fully relax on the experimental or simulation time scale. In the case of simulation, we run the system for 10^5 simulation time units and sampled for a further 10^5 time units except in the "very dense" case (h). There we run the system for 5×10^5 time units and sample for a further 5×10^5 time units.

D. Mapping state points between experiment and simulation

Despite screening the residual electrostatic charge with tetrabutylammonium bromide salt, some repulsion between the colloids can remain. Although in the system with smaller particles [gelation $(\overline{ba})$ path in Fig. 1], the electrostatics are weak and neglected,[42] in the system with larger colloids which we use for the "hard" sphere $(\overline{bd})$ and dense $(\overline{dc})$ paths in Fig. 1, we treat the electrostatic repulsions as a Yukawa interaction $u_Y(r) = \varepsilon_Y \exp[-\kappa\sigma(r/\sigma - 1)]/(r/\sigma)$. We set $\varepsilon_Y = k_B T$ and the Debye length κ^{-1} is taken as 100 nm, following Ref. 42. We map the system to hard spheres, using the Barker-Henderson effective hard sphere diameter $\sigma_e = \int_0^\infty dr[1 - \exp(-\beta u(r))]$, where $\beta = 1/k_B T$ such that the effective packing fraction $\phi_e = \phi(\sigma_e/\sigma)^3$. This increases ϕ_e by around 8% relative to the absolute packing fraction ϕ (note that in the simulations, $\phi_e = \phi$).

Previously, we have shown that the Asakura-Oosawa (AO) potential describes the polymer-induced attractions between the colloids rather well.[42] Furthermore we have obtained good agreement with the experiment by assuming simple addition of AO and strongly screened Yukawa interactions for similar conditions to those we employ here.[59] We therefore make the same assumption that the colloid-colloid interaction is described by the sum of the AO and Yukawa interactions (for details see Ref. 42) and map these to the square well model with well width 3% and depth ε, using the extended law of corresponding states.[60] This requires that the reduced second virial coefficient $B_2^* = 3/\sigma_e^3 \int_0^\infty dr\, r^2[1 - \exp(-\beta u(r))]$ is matched between the assumed experimental potential and the square well. One expects this approach to work up to polymer concentrations

even beyond the overlap concentration c_p^*.[61] The highest we encounter is $0.51 c_p^*$ so we conclude that the mapping of state points should be accurate here.

The error in colloid volume fraction can be as large as 6%[44,62] (which we assume in Fig. 1). However, we note here that the mapping to simulation [Fig. 3(a)] allows us to be rather more confident about the *effective* volume fraction. Figure 3(a) indicates that the errors in ϕ_e are comparable to or smaller than the symbols. On the other hand, the error in polymer concentration is determined from the fluid-gel transition. For the error in mapping c_p to ε, again we appeal to comparisons with simulation, Figs. 3(d) and 3(e). For gelation [path $(\overline{ba})$ in Fig. 1], the agreement is again very good. For the dense gel [path $(\overline{dc})$], there is some discrepancy for low values of c_p. While the mapping of slightly charged colloids and weak polymer attractions to the attractive square well is an interesting problem, and similar behavior to that we observe has been encountered before in an almost identical experimental system,[63] this has no effect on our conclusions and we leave a detailed analysis for future work.

E. Topological cluster classification (TCC) analysis

For the topological cluster classification (TCC) analysis of the local structure, we use a simple bond criterion to define the bond network.[64,65] Setting a bond length in this way is appropriate for dilute gels where particles in a network may have no close neighbors on one side [Fig. 1(b)].[65] An appropriate bond length is the first minimum of $g(r)$. However our polydisperse systems necessitate a further constraint, namely, that two large particles may touch. This is readily implemented in simulation where the particle size is known. We use the same
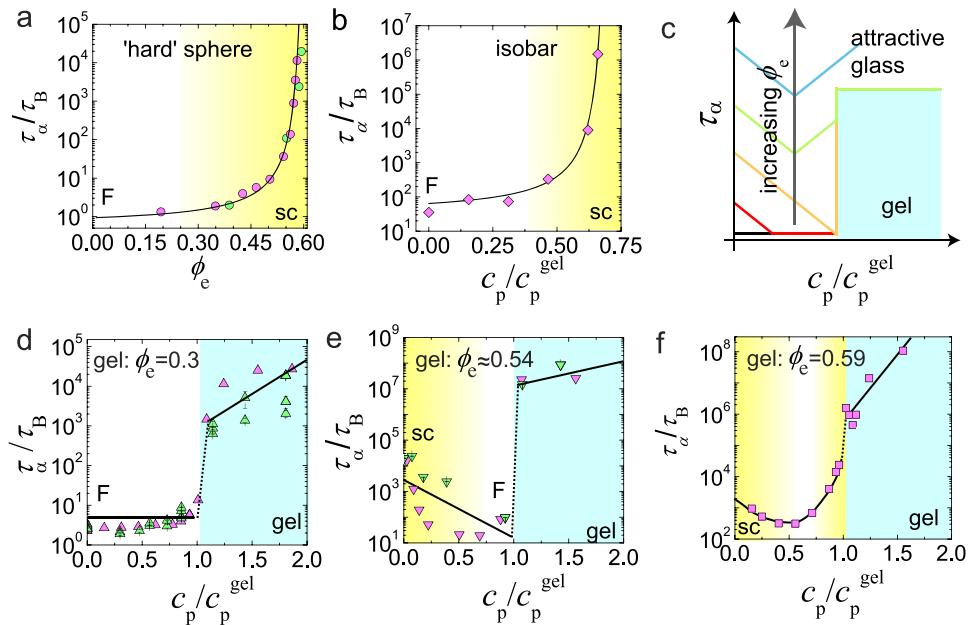
FIG. 3. Structural relaxation time τ_α along the paths in Fig. 1 showing the continuous approach to vitrification and discontinuous gelation. (a) Path $\overline{bd}$ indicating the continuous nature of the approach to the hard sphere glass. (b) Isobaric path showing no re-entrant dynamics. (c) Schematic of the gelation behavior at different colloid volume fractions as indicated by the colored lines. (d)–(f): Gelation at increasing volume fraction. (d): $\phi_e = 0.35$, path $(\overline{ba})$; (e): $\phi_e \approx 0.54$, path $(\overline{dc})$; (f): $\phi_e = 0.59$, dashed path in Fig. 1. In (a) and (b), the lines are VFT fits. In (d)–(f), the lines are to guide the eye. Experiment and simulation data are scaled such that "hard" spheres agree (see Sec. II D). Green symbols are experimental data, and pink symbols are simulation data. "F" and "sc" denote fluid and supercooled liquid, respectively. $\tau_B = \pi\eta\sigma^3/8k_B T$, the time taken for a particle to diffuse its own radius at infinite dilution in a solvent of viscosity η. Dotted lines denote quasi-discontinuous jumps in relaxation time at gelation. The error bars in the value for τ_α are obtained from fitting the ISF data (see Fig. 2).

criterion for the experiments, noting that there the polydispersity is 2% less and that therefore, although the particle size distribution is continuous, the number of large-large bonds lost is very small. Moderate changes in the bond length criterion or indeed using a modified Voronoi construction with a maximum bond length[64] had no impact on our findings. We assign each particle to the largest cluster in which it is found.[65]

Our analysis is sensitive to crystallisation,[54,66] and this can be encountered in gels and glass-forming systems.[47,54,56,67] Here we find only trace quantities of particles identified in crystalline environments and attribute this to the (weak) polydispersity.[54]

III. RESULTS AND DISCUSSION

A. Phase diagram

In order to tackle the dynamic arrest scenarios, we need the equilibrium phase diagram. As noted above, this is disputed.[11,19] Therefore we begin by showing the phase diagram of our system that we have determined in Fig. 1. Here we use the effective volume fraction of colloids ϕ_e and the attraction strength ε (i.e., polymer concentration c_p) as the control parameters. The phase diagram is determined by allowing a system at $\phi_e \approx 0.3$ to phase separate in simulation. We then directly determine the density in each phase by fitting a hyperbolic tangent function to the density across the simulation box.[68] We take the critical point from literature data.[41]

Regarding the lifetimes of the states observed, the crucial point is that the characteristic time of the experimental protocol (~30 min) is much longer than the time scale of demixing and the resulting dynamical arrest to form a gel, but much shorter than the gel lifetime. We return to the aging dynamics in Sec. III G. Therefore each state point is rather well defined and may be compared with simulations. In connection with thermodynamics, it is possible to draw a line which distinguishes gels and glasses, under the premise that gelation is driven by the spinodal decomposition above. This is the liquid-gas spinodal. But first, we need to address the suggestion that percolation drives gelation.[17] To do this, we estimate percolation and plot the percolation threshold in Fig. 1. In Sec. III B, we examine the dynamics of the system in some detail, but for now, we observe that percolation has no discernible effect on the dynamics and we henceforth conclude that percolation is a necessary but not a sufficient condition for gelation in this system. We acknowledge that a finite size scaling study of percolation would yield a more accurate result, but we argue that the analysis we have performed is sufficient for our purposes and leave a more detailed investigation for the future.

Thus we identify gelation with spinodal phase separation *provided the colloid-rich phase has sufficient density to drive dynamical arrest*. We therefore plot the liquid-gas spinodal, noting that here it is indistinguishable from the binodal separating the thermodynamically stable and unstable regions. The critical point is determined from literature data,[41] and the phase boundary is determined from our simulations. We find that for very weak quenches below the critical point, on long time scales, the simulations do fully demix. That is to say, on

the simulation time scale, the gel is metastable to full liquid-gas demixing. We emphasise that this only occurs for temperatures very close to criticality (less than 10%) and that we do not observe this behavior in the experiment. This demixing brings the volume fraction of the colloid-rich phase to higher values ($\phi_e \approx 0.59$) than those obtained in previous simulations[19,69] but in line with indications from some experiments.[11,37] Thus our results indicate that the demixed liquid is sufficiently dense for dynamical arrest. The proximity of the values of ε for the critical point and fully demixed liquid with $\phi_e \approx 0.59$ indicates that the binodal must be almost flat in the ϕ_e, ε representation. *Our first result is to confirm spinodal decomposition rather than percolation as the mechanism for gelation.*

This formation of a very dense colloid-rich phase is common to a wide range of colloid volume fractions because the phase separation line is almost flat. The important observation here is that across this range of colloid volume fractions, one expects to cross the phase separation line at almost the same effective temperature (criticality), which corresponds to $\varepsilon^* = 3.22\, k_B T$ for the 0.03σ square well.[41] In the experiments, we denote the polymer concentration required for gelation as c_p^{gel} which we take as the midpoint of the highest fluid c_p and lowest gel c_p as previously.[65] While "liquids" of spheres at $\phi_e \approx 0.59$ are in principle metastable to crystallization, in our system, this is totally suppressed by polydispersity. Thus, having determined the state diagram and resolved discrepancies in the literature,[11,17,19,37] we are in a position to tackle the dynamical behavior in this important model system.

To elucidate the different dynamical arrest scenarios, we consider the following paths through the state diagram indicated in Fig. 1: $(\overline{bd})$: increasing packing fraction along the "hard sphere" line (with no added polymers) leads to vitrification; $(\overline{ba})$: at a relatively low colloid volume fraction ($\phi_e = 0.35$), addition of polymer results in gelation at a polymer concentration c_p^{gel};[65] $(\overline{dc})$: addition of polymers at high colloid density leads to a transition between two states with slow dynamics, with an "ergodic pocket" in between reminiscent of that observed previously.[27] Thus glass [Fig. 1(d)] and gel [Fig. 1(c)] are found even at comparable volume fraction. *Our second main finding is that since the liquid-gas coexistence region of the phase diagram corresponds to gelation, far from being a low-density network, gels can be found at high volume fractions.* We shall see below that gels have local and topological structures distinct from supercooled liquids at the same volume fraction, although at a superficial level both have similar disordered structures with homogeneous density on a longer length scale.

B. Dynamics

Next we focus on the dynamical behavior associated with these paths. In Fig. 3, we show the structural relaxation time τ_α (see Sec. II C) along the paths in Fig. 1. The hard sphere glass transition [path $(\overline{bd})$] exhibits a continuous increase in τ_α as shown in Fig. 3(a). Both experiment and simulation data are well described by the Vogel-Fulcher-Tammann (VFT) relation $\tau_\alpha = \tau_0 \exp[D\phi_e/(\phi_0 - \phi_e)]$, where τ_0 is a relaxation time in the normal liquid, D is the "fragility index," and $\phi_0 \approx 0.61$ is the ideal glass transition volume fraction.[24] For

$\phi_e \gtrsim 0.59$, structural relaxation does not occur on our time scales, so hard spheres at these high densities are glasses for our purposes.

This vitrification behavior contrasts strongly with paths which cross the liquid-gas phase separation line [see Figs. 3(d)–3(f)]. All of these gelation paths exhibit a discontinuity in τ_α as the line is crossed at $c_p/c_p^{gel} = 1$. Although aging and the nature of the dynamics (Brownian) with hydrodynamic interactions for the experiments and Newtonian for the simulations lead to some variation in the value of τ_α in non-ergodic gel states, the discontinuity of τ_α upon gelation is robust (see Fig. 3). These results reflect the fact that gelation is a discontinuous transition between a fluid and a gel which occurs at the phase separation line for a wide range of colloid volume fractions. This is consistent with previous work[8–11,27] which identified gelation with (arrested) spinodal phase separation, but we would not expect this behavior if we assumed that gelation was driven by percolation.[17] Here we emphasize the dynamic manifestation of gelation—a quasi-discontinuous jump in the relaxation time from an ergodic fluid to a non-equilibrium state. *This discontinuous nature of gelation* forms our third finding and constitutes the basis of the dynamic distinction between gelation and vitrification. Below we go further to explore the consequences of this spinodal gelation at high particle volume fractions.

At $\phi_e \approx 0.54$, upon increasing the attraction strength, the phase separation line is crossed and thus a gel rather than an attractive glass is formed. This is evidenced by a discontinuous jump of six orders of magnitude in relaxation time upon crossing the phase separation line [see Fig. 3(e)]. On the other hand, for ϕ_e greater than the dense side of the phase separation region, which we estimate as $\phi_e \gtrsim 0.59$, we expect an attractive glass rather than a gel, as the line is not crossed. In the border composition region, however, the distinction between gels and glasses is not always so clear. Thus it is possible that some work previously thought to pertain to a re-entrant glass transition in fact concerned gelation which may be preceded by a supercooled liquid. In other words, in the absence of the phase diagram which our work provides, it has not been possible—until now—to distinguish a gel (having crossed the spinodal) and an attractive glass.

C. The spinodal limit of the attractive glass

We now address the interplay between spinodal gelation and the attractive glass transition. The state diagram in Fig. 1 shows that gels can form at high volume fraction. Re-entrant dynamics along lines similar to path ($\overline{dc}$) have previously been identified with an "attractive glass."[2,27,28] Now an attractive glass is predicted by mode-coupling theory (MCT) at high colloid volume fraction,[27,70] but the predicted attraction strength at arrest varies considerably from that found in simulation;[28] moreover, distinguishing vitrification and (spinodal) gelation is not easy with MCT. Computer simulations indicate that at sufficiently high colloid volume fractions, systems with attractions fail to relax fully on accessible time scales.[22] As shown in Fig. 3(f), our analysis reveals a new sequence of states upon increasing c_p: a hard sphere supercooled liquid, fluid (attractive), supercooled liquid which is

interrupted by gelation. One may, at this point, enquire as to what might have happened to the attractive glass. Our work suggests that it is not found at $\phi_e = 0.59$, which suggests that it may reside at higher volume fractions. We return to this issue in Sec. III D.

We summarize our findings of the relaxation time in the fluid-gel transition in Fig. 3(c). At low densities, the system is mobile until $(c_p/c_p^{gel} \approx 1)$, at which point it undergoes discontinuous dynamical arrest. Increasing colloid volume fraction leads to re-entrant dynamical behavior as a function of increasing attraction once ϕ_e is sufficient that hard spheres exhibit slow dynamics. The fluid-gel transition remains abrupt. Upon increasing volume fraction further ($\phi_e \to 0.59$), the gel transition is preceded by a supercooled liquid. *Our fourth major finding is that we see hints of the attractive glass transition,[27] but this is ultimately superseded by gelation.* We emphasize that both experiments and simulations show exactly the same behavior. Although equilibrium or metastable states might be reasonably well modeled by MD simulation,[71] the nature of the dynamics can be important in gelation.[72,73] Nevertheless, in Figs. 3(d) and 3(e), we find good agreement between experiment and simulation.

D. Isobaric quenches avoid gelation

In the above, we have argued that gels should persist even up to colloid volume fractions $\phi_e \gtrsim 0.59$ and now give further weight to this claim. If indeed the phase separation line is crossed, quantities such as the (osmotic) pressure may feature a discontinuity. Note that here we are considering an effective one-component system of colloids. Contributions from the polymer are integrated out.[43] From our simulations, we compute the pressure for the paths in Fig. 1. As expected, discontinuities are found upon crossing the phase separation line, up to $\phi_e = 0.59$ (pressure is shown in Fig. 4). In fact, for $\phi_e \lesssim 0.54$, the pressure turns negative. This provides evidence that the dense side of the phase-separation line lies at $\phi_e \gtrsim 0.59$. The consequences for the re-entrant glass transition are considerable: for $\phi_e \lesssim 0.59$, gelation will intervene after the system passes through a supercooled liquid regime [see Figs. 3(e) and 3(f)]. In other words, for $\phi_e \lesssim 0.59$, the re-entrant glassy state becomes a gel when $c_p \gtrsim c_p^{gel}$. Furthermore, $\phi_e = 0.59$ is a *lower bound* for the high-density limit of gelation: in equilibrium, the high-density side of the phase separation line may be denser still.
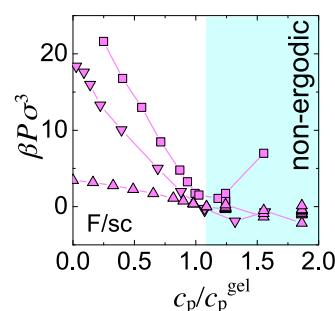
FIG. 4. Pressure upon quenching sticky spheres at various packing fractions. Up triangles are "gels," path ($\overline{ba}$), down triangles are "dense gels," path ($\overline{dc}$), and squares are "very dense" (dashed line) in Fig. 1. Simulation data.

That the (osmotic) pressure exhibits such a discontinuity leads to the hypothesis that constant-pressure paths through the phase diagram cannot produce a gel. Therefore, dynamic arrest upon quenching should in this case correspond to the attractive glass. We therefore carried out simulations at fixed pressure ($15.45\,k_BT\sigma^{-3}$) which corresponds to the isobar indicated as a dotted line in Fig. 1. Since such a path should not produce a gel, we expect no discontinuity; and in Fig. 3(b), we indeed find a continuous increase in relaxation time as a function of attraction strength. The VFT fit in Fig. 3(b) indicates divergence at $c_p/c_p^{gel} = 0.709$, in contrast to the quenches at constant volume, all of which show a sudden slowdown in dynamics at $c_p/c_p^{gel} \approx 1$. Moreover, the isobar in Fig. 1 shows a departure to very high densities, so the system avoids gelation and undergoes vitrification. Thus, at gelation (where the pressure tends to negative values) the system cannot support external stress (pressure). Gels are found exclusively in soft materials formed of a mixture whose components have large size disparity.[16] Although possible,[74] molecular systems have not so far undergone spinodal gelation. Soft matter experiments are typically carried out at constant volume, while in molecular systems, pressure is often fixed. The equivalent to isobaric quenching would be constant osmotic pressure of the effective one-component colloid system. Were such experiments to be performed, we expect no gelation. *Our fifth finding is that gelation and (osmotic) pressure are intimately coupled. Fixing the pressure prevents gelation, leaving vitrification to an attractive glass as the only route of arrest available.*

E. Structure

The dynamics and phase behavior provide a means by which gelation and vitrification may be distinguished. We now show that local structural measures also support the idea of gelation as a discontinuous transition to a state far from equilibrium. While density-density correlations show little change upon vitrification,[1,4] here we find that gelation exhibits rather different behavior.

Since gels are associated with demixing, upon crossing the phase separation line, we expect the first minimum of the pair correlation function $g(r)$ to move to a value close to contact (σ) reflecting condensation.[26] Indeed this behavior is found: in Figs. 5(a) and 5(b), the first minimum of $g(r)$ is indicated by arrows for the hard sphere glass transition and gelation, respectively. The latter case shows a distinct jump around the phase separation line $c_p/c_p^{gel} = 1$, while for hard spheres, the minimum should and does decrease *continuously* upon increasing density. The resulting $g(r)$ minima are plotted as a function of ϕ_e and c_p/c_p^{gel} in Figs. 5(c) and 5(d), respectively, where they are labeled as min[$g(r)$]. Discontinuous behavior is seen at all ϕ_e for the gels, while in hard spheres, both experiments and simulations show a continuous fall in min[$g(r)$] as a function of ϕ_e. We believe the reason this was not observed before may be related to our analysis in real space rather than reciprocal space[75] and particle tracking in 3D rather than 2D.[29]

The particle-level detail in our experiments also enables us to detect small voids inaccessible to other techniques. To
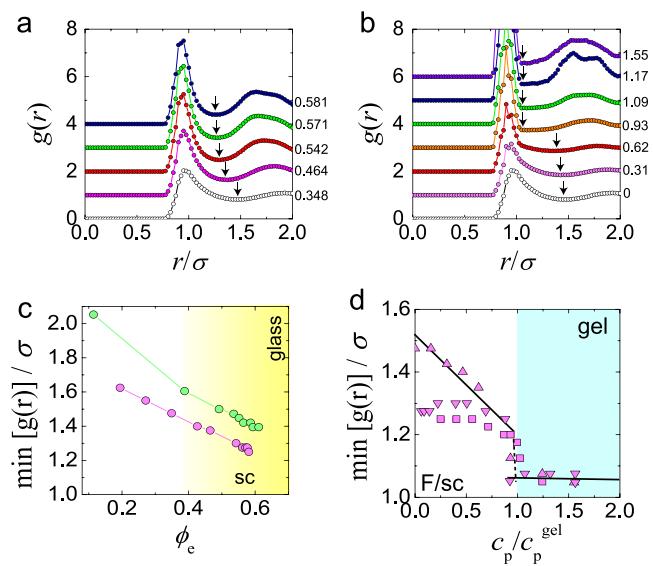
FIG. 5. Distinguishing gelation and vitrification via the radial distribution function $g(r)$. (a) $g(r)$ for different ϕ_e for hard spheres with arrows indicating first minima. Data are labeled by ϕ_e. Green data are experiment, and pink data are simulation. (b) $g(r)$ along path ($\overline{ba}$) in Fig. 1 with arrows indicating the first minima. Data are labeled with c_p/c_p^{gel}. Simulation data. (c) The first minimum of $g(r)$ as a function of ϕ_e. (d) The first minimum of $g(r)$ for state points along paths in Fig. 1. The three paths indicated in Fig. 1 by [($\overline{ba}$), gel], [($\overline{dc}$), dense gel], and (dashed line, very dense gel) are shown in (d) as down triangles, up triangles, and squares, respectively. In (a) and (b), data are offset for clarity.

reveal such voids, we apply a Gaussian blur of standard deviation 0.2σ to an image of spheres of diameter σ reconstructed from coordinate data. As shown in Fig. 6(b), these are present in the gel, even though its high volume fraction ($\phi_e = 0.54$) prevents larger scale demixing, but are almost absent from hard spheres at the same density [Fig. 6(a)]. Similar behavior may be observed in Figs. 1(c) and 1(d). This tells us there is a difference in the topology between supercooled liquids and gels: homogeneous vs. topology with largely negative Euler characteristics. Apart from voids much smaller than the particles, supercooled liquids are homogeneous whereas gels have a number of voids (or holes) larger than the particles.

To further probe the local structure, we use the topological cluster classification (TCC), which identifies structures whose bond network is equivalent to clusters that minimize the potential energy in isolation.[65] The TCC considers clusters of size $5 \leq m \leq 13$, along with HCP and FCC crystalline configurations of 13 particles. In the case of "hard" spheres, the relevant parameter is volume and the same set of clusters is appropriate to minimize the free volume.[66] For all systems we consider here, we use the clusters shown in Figs. 6–8. Details are provided in Sec. II E.

In the experimental data rendered in Figs. 6(c) and 6(d), particles are colored according to their TCC structure. For the supercooled liquid [Fig. 6(c)], we see a considerable number of particles rendered in green associated with ten-membered defective icosahedra which are based on five-membered rings, while for the gel [Fig. 6(d)], we see predominantly five-membered clusters formed from two tetrahedra (white). Thus the two states, supercooled liquids and gels, have distinct local
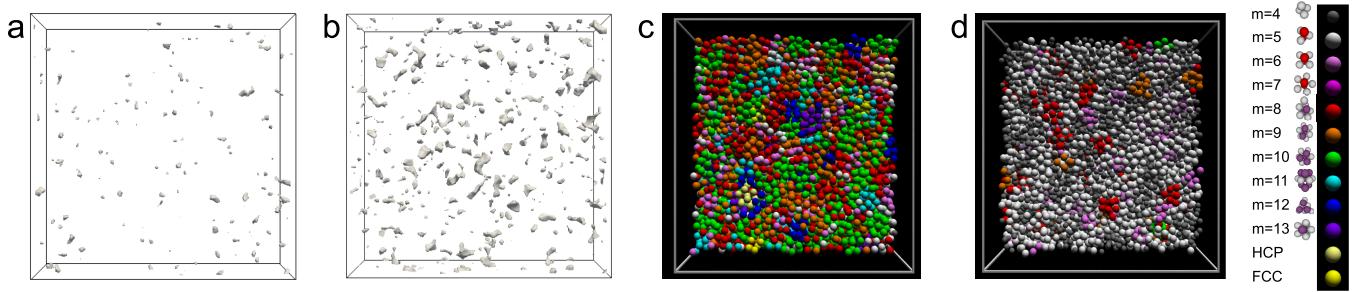
FIG. 6. Structural differences between glasses and gels at similar volume fraction. (a) Voids in "hard" spheres ($\phi_e = 0.54$). (b) Voids in dense gel ($\phi_e = 0.54$, $c_p/c_p^{gel} = 1.43$). Experimental data. (c) and (d): Experimental data rendered following the topological cluster classification for "hard" sphere supercooled liquid ($\phi_e = 0.59$) and dense gel ($\phi_e \approx 0.54$, $c_p/c_p^{gel} = 1.08$), respectively. Local structures considered in the TCC are indicated on the right.
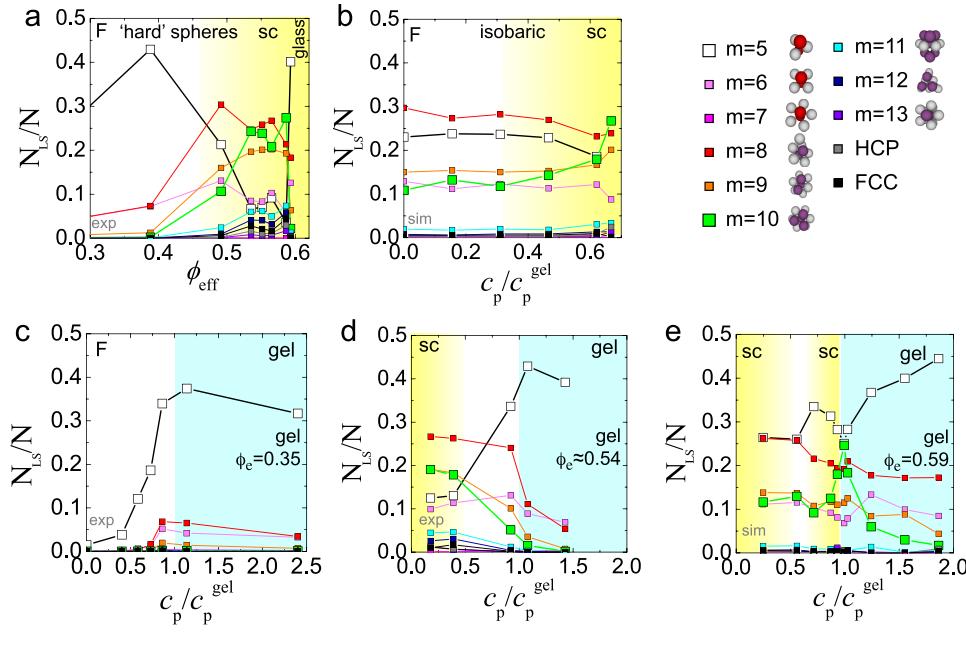
FIG. 7. Topological cluster classification of glass and gel transitions. Populations of local structures N_{LS}/N are plotted along paths in Fig. 1. Vitrification along the paths in hard spheres ($\overline{bd}$) (a) and at constant pressure (b). These are contrasted with gelation (c)–(e). (c) $\phi_e = 0.35$; (d) $\phi_e \approx 0.54$; (e) $\phi_e = 0.59$. Local structures considered in the TCC are indicated on the right. Colored lines correspond to different structures identified by the TCC and specified in the legend. sc denotes supercooled liquid.
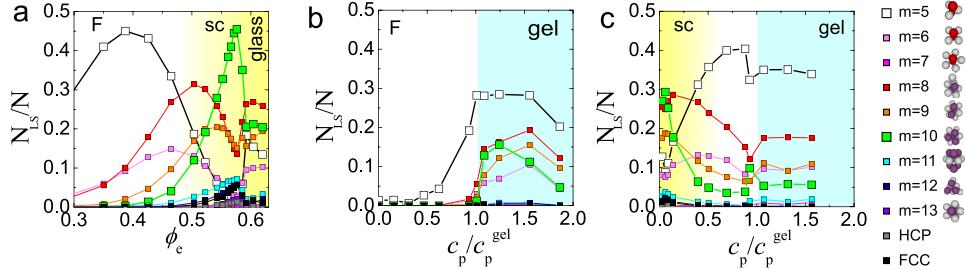
FIG. 8. Topological cluster classification analysis for simulation data. Population of local structures N_{LS}/N, mapped to the following paths in Fig. 1: (a) hard spheres; (b) "gel;" (c) "dense gel." They correspond to the plots in Figs. 7(a), 7(c), and 7(d), respectively.

structure, even though they are at the same volume fraction and appear similar. If we consider the response of the local structure to vitrification [Fig. 7(a)], we see a gradual, continuous change up to the hard sphere glass transition ($\phi_e \approx 0.59$). The $m = 10$ defective icosahedron dominates the system just prior to vitrification. Simulations show similar behavior (see Fig. 8). Interestingly, quenching along the isobaric path also shows an increase in the same local structure, the defective icosahedron [Fig. 7(b)].

By contrast, in the case of gelation at moderate density [path ($\overline{ba}$)], Fig. 7(c) shows a sharp rise in cluster population. Not only is the rise in population of local structures very sudden

but also the structure involved is different: gels are dominated by five-membered bitetrahedra. The same holds for higher density in the case of path ($\overline{dc}$) [Fig. 7(d)], although here the fluid is sufficiently dense that its own population of local structures is considerable. Data from simulations of the "gel" and "dense" paths show similar behavior (see Fig. 8). Thus upon gelation, the larger structures associated with denser fluids give way to $m = 5$ clusters as discussed above. Remarkably, at $\phi_e = 0.59$, Fig. 7(e) shows behavior indicative of both vitrification and gelation consistent with our analysis above. In the supercooled liquid which precedes gelation, there is a strong rise in the $m = 10$ defective icosahedron associated with

vitrification. However, for attractions greater than those required for gelation, the structure reverts immediately to the $m = 5$ triangular bipyramid. This mirrors Fig. 3(f) where we see a supercooled liquid prior to gelation.

F. Local structure far from equilibrium

What drives the system to select between the $m = 5$ bitetrahedron and $m = 10$ defective icosahedron? We offer the following explanation. Equilibrated hard sphere supercooled liquids exhibit high populations of defective icosahedra.[76] By contrast, due to rapid densification associated with phase separation, gels become arrested at times much shorter than the structural relaxation time. Thus the particles have no chance to organize into larger $m = 10$ defective icosahedra but remain in the structure formed immediately upon compression. We argue that local structure in highly non-equilibrium states should be based on tetrahedra. Tetrahedra, which are the basic rigid arrangement of spheres in 3D, are formed at short times. This also holds for the $m = 5$ bitetrahedra, whereas organization of the tetrahedra into larger clusters is suppressed due to dynamical arrest. Thus the system is unable to reach a locally equilibrated configuration, for which formation of larger clusters is expected.

We can test the hypothesis that highly non-equilibrium states unable even to relax locally are dominated by tetrahedra, by considering a hard sphere glass. We expect that these should also dominate the glass—unlike the supercooled fluid where relaxation occurs on the experimental time scale. This is precisely what we find, both in experiments [Fig. 7(a)] and simulation [Fig. 8]. This situation is similar to hyperquenching of molecular glassformers. Thus we identify a structural motif to distinguish systems where local relaxation can occur and where it cannot. This can be used as a measure for how far from equilibrium the system is.

G. Aging in gels and the role of dynamics

Aging dynamics are shown in Fig. 9 for a gel in simulation with $\phi_e = 0.35$ and $c_p/c_p^{gel} = 1.86$. We estimate that an equilibration time of $1000\tau_B$ is comparable to the experimental waiting time. The discussion in Secs. III E and III F leads us to

expect a tendency towards the defective icosahedron structure upon aging. Indeed at very long times, in simulation gels show a tendency towards defective icosahedra and so in gels some reorganization can take place eventually.

We now consider the effect of the choice of dynamics on aging. In equilibrium, our MD data might be expected to provide a reasonable description of the experiments, on time scales where particles have undergone sufficient collisions that their momentum has become uncorrelated. Out of equilibrium, the situation changes, and the nature of the dynamics can strongly influence the behavior of the system.[72,73]

We see in the ISFs plotted in Fig. 9(a) that longer waiting times indeed result in an increase in the structural decay time but that this increase is around a factor of three for an order of magnitude increase in the waiting time. This lies within the scatter in Figs. 2(d) and 2(e) where the experiment and simulation are compared. We saw no significant aging effects in our experiments. In Fig. 9(b), we show a TCC analysis for the structural evolution of the gel. Only at time scales greater than $3 \times 10^5 \tau_B$ is there a significant change in local structure which is around the limit of the experimental time scale. We believe that any difference in behavior between experiment and simulation is related either to the nature of the dynamics or to the effective interactions. The dynamics can lead to significant differences in structure between experiment and simulation.[72,73] However details in the interactions may also be important. In particular, rotation of the particles around one another may be suppressed in the experiments relative to the simulations.[77]

IV. GENERALITY

We now consider the consequences of our work for other systems. It is known that polymer solutions,[15] clay suspensions,[78] and protein solutions[13,14] show behavior compatible with spinodal gelation. All have strong dynamic asymmetry between the two components, and accordingly all exhibit viscoelastic phase separation similar to colloidal suspensions described here,[10,16,78] so we expect that our findings should also apply to these systems, which should take place if viscoelastic phase separation occurs. We further note that similar phenomenology is seen in active matter, where activity can play the role of attraction leading to two-body correlations reminiscent of Fig. 5(b).[79] Finally, we remark that a system in which phase separation is formally absent (for example, patchy particles[80] or one with competing interactions[33]) would be an interesting testing ground for the attractive glass transition without the influence of gelation. It is possible in principle to tune interactions continuously from the sticky spheres studied here, either to systems of competing interactions[33] or to patchy particles.[5–7] In the case of patchy particles in particular, dynamics are strongly coupled to percolation, unlike what we have found here. Given that the interactions can be tuned continuously, which leads to a continuous shift in phase boundaries, we expect that the coupling between spinodal decomposition and percolation will also shift continuously, with the former driving arrest for sticky spheres and the latter for patchy particles.

FIG. 9. Aging in gels. (a) Intermediate scattering functions from simulation data for $\phi_e = 0.35$ and $c_p/c_p^{gel} = 1.864$. Different waiting times are expressed in units of the Brownian time. Here the results from simulation (black lines) are fitted with a stretched exponential (grey lines) as described in the main text. (b) TCC analysis of the structural evolution as a function of waiting time t_w. TCC structures are detailed in Fig. 7.

V. CONCLUSIONS

In conclusion, we have confirmed spinodal decomposition as the mechanism for gelation in sticky spheres. This enables us to show that gelation and vitrification in an important model system may be distinguished by the quasi-discontinuous nature of the former and the continuous nature of the latter as a function of density and attraction, which controls the dynamics. In order to do this, we have considered dynamical pathways and cleared up discrepancies in the literature concerning the phase diagram[11,19,37] and the role of percolation.[17] The discontinuity in gelation manifests itself both in dynamical and structural properties, namely, the relaxation time τ_α, and local particle configuration. Underlying this behavior is that gelation involves a thermodynamic transition (phase separation), which leads to rapid densification and hyperquenching.

Thus, gelation and vitrification are readily distinguished in sticky spheres by measuring dynamical or structural quantities along paths in the (ϕ_e, ε) plane. We reveal a previously unidentified path of fluid-supercooled liquid-gel for $\phi_e = 0.59$. Thus certain states identified as glasses previously[31] may in fact be gels which may explain some previously observed differences between experiment and simulation.[81]

Moreover the topological cluster classification reveals a clear structural signature of systems which fail to relax. In the case of gels of sticky spheres and rapidly compressed hard sphere glasses, the structure is dominated by small tetrahedra, while supercooled liquids exhibit larger ten-membered defective icosahedra which form at times longer than the structural relaxation time. That the larger structures require structural relaxation to form means that the smaller structures based on tetrahedra are related to "hyperquenching" or states very far from equilibrium. Since this disorder is related to rapid densification upon (arrested) phase separation, colloidal gels should—and do—share local structures with rapidly compressed hard sphere glasses and poses a question as to the role of aging. In fact, by considering an aging system, we show the local structure approaches that are found in equilibrated supercooled liquids. We expect that this behavior may have some universality which could be explored in other glass-forming systems such as metallic glasses.

A significant question our work opens is to understand why some experiments do find very strong dynamic slowing upon percolation.[17] One possibility is that the model system used (of silica with grafted polymers in which the attractions are driven by the solubility of the polymer and *not by depletion*) is different from the sticky sphere behavior somehow. While the thermodynamic behavior of this system is well known, and closely reproduces that of sticky spheres,[82] it is possible that some dynamic effects of the breaking of "bonds" between neighboring particles differ from the experiments and simulations here. Another aspect is that at low volume fractions ($\phi \lesssim 0.01$), percolation takes some time to occur even in the demixing region of the phase diagram.[83,84] Under these conditions, percolation does control gelation.

We observe phase separation with the unusually high "liquid" volume fraction of 0.59. This prompts further work to explore how dense the liquid can become and investigations of the attractive glass in systems where it is not influenced by demixing. We have highlighted the role of pressure in gelation and shown that quenching at constant volume is necessary for gelation and explains its prevalence in soft matter. This motivates experiments where osmotic pressure is fixed to test this prediction. Such experiments could be done by using a membrane through which polymer molecules pass.

Concerning the attractive glass, our work suggests that this is obtained upon constant pressure quenching. We find evidence of an attractive glass by using an isobaric path through the phase diagram that skirt around the edge of the gel at volume fractions $\phi \gtrsim 0.59$.

[1] L. Berthier and G. Biroli, "Theoretical perspective on the glass transition and amorphous materials," Rev. Mod. Phys. **83**, 587–645 (2011).

[2] W. C. K. Poon, "The physics of a model colloid-polymer mixture," J. Phys.: Condens. Matter **14**, R859–R880 (2002).

[3] E. Zaccarelli, "Colloidal gels: Equilibrium and non-equilibrium routes," J. Phys.: Condens. Matter **19**, 323101 (2007).

[4] C. P. Royall and S. R. Williams, "The role of local structure in dynamical arrest," Phys. Rep. **560**, 1 (2015).

[5] E. Bianchi, J. Largo, P. Tartaglia, E. Zaccarelli, and F. Sciortino, "Phase diagram of patchy colloids: Towards empty liquids," Phys. Rev. Lett. **97**, 168301 (2006).

[6] I. Saika-Voivod, H. M. King, P. Tartaglia, F. Sciortino, and E. Zaccarelli, "Silica through the eyes of colloidal models-when glass is a gel," J. Phys.: Condens. Matter **23**, 285101 (2011).

[7] S. Biffi, R. Cerbinoa, F. Bomboi, E. M. Paraboschia, R. Asselta, F. Sciortino, and T. Bellini, "Phase behavior and critical activated dynamics of limited-valence DNA nanostars," Proc. Nat. Acad. Sci. U. S. A **110**, 15633–15637 (2013).

[8] R. Piazza and G. Di Pietro, "Phase separation and gel-like structures in mixtures of colloids and surfactant," Europhys. Lett. **28**, 445–450 (1994).

[9] N. A. M. Verhaegh, D. Asnaghi, H. N. W. Lekkerkerker, M. Giglio, and L. Cipelletti, "Transient gelation by spinodal decomposition in colloid-polymer mixtures," Phys. A **242**, 104–118 (1997).

[10] H. Tanaka, "Viscoelastic model of phase separation in colloidal suspensions and emulsions," Phys. Rev. E **59**, 6842–6852 (1999).

[11] P. J. Lu, E. Zaccarelli, F. Ciulla, A. B. Schofield, F. Sciortino, and D. A. Weitz, "Gelation of particles with short-range attraction," Nature **435**, 499–504 (2008).

[12] H. Tanaka and Y. Nishikawa, "Viscoelastic phase separation of protein solutions," Phys. Rev. Lett. **95**, 078103 (2005).

[13] F. Cardinaux, T. Gibaud, A. Stradner, and P. Schurtenberger, "Interplay between spinodal decomposition and glass formation in proteins exhibiting short-range attractions," Phys. Rev. Lett. **99**, 118301 (2007).

[14] T. Gibaud, F. Cardinaux, J. Bergenholtz, A. Stradner, and P. Schurtenberger, "Phase separation and dynamical arrest for particles interacting with mixed potentials-the case of globular proteins revisited," Soft Matter **7**, 857–860 (2010).

[15]R. M. Hikmet, S. Callister, and A. Keller, "Thermoreversible gelation of atactic polystyrene: Phase transformation and morphology," Polymer **29**, 1378–1388 (1988).

[16]H. Tanaka, "Viscoelastic phase separation," J. Phys.: Condens. Matter **12**, R207 (2000).

[17]A. P. R. Eberle, N. J. Wagner, and R. Castaneda-Priego, "Dynamical arrest transition in nanoparticle dispersions with short-range interactions," Phys. Rev. Lett. **106**, 105704 (2011).

[18]M. Kohl, R. Capellmann, M. Laurati, S. Egelhaaf, and M. Schmiedeberg, "Directed percolation identified as equilibrium pre-transition towards non-equilibrium arrested gel states," Nat. Commun. **7**, 11817 (2016).

[19]M. A. Miller and D. Frenkel, "Competition of percolation and phase separation in a fluid of adhesive hard spheres," Phys. Rev. Lett. **90**, 135702 (2003).

[20]K. N. Pham, G. Petekidis, D. Vlassopoulos, S. U. Egelhaaf, P. N. Pusey, and W. C. K. Poon, "Yielding of colloidal glasses," Europhys. Lett. **75**, 624–630 (2006).

[21]N. Koumakis and G. Petekidis, "Two step yielding in attractive colloids: Transition from gels to attractive glasses," Soft Matter **7**, 2456–2470 (2011).

[22]E. Zaccarelli and W. C. K. Poon, "Colloidal glasses and gels: The interplay of bonding and caging," Proc. Nat. Acad. Sci. U. S. A **106**, 15203–15208 (2009).

[23]A. Puertas, M. Fuchs, and M. Cates, "Comparative simulation study of colloidal gels and glasses," Phys. Rev. Lett. **88**, 098301 (2002).

[24]G. Brambilla, D. El Masri, M. Pierno, L. Berthier, L. Cipelletti, G. Petekidis, and A. B. Schofield, "Probing the equilibrium dynamics of colloidal hard spheres above the mode-coupling glass transition," Phys. Rev. Lett. **102**, 085703 (2009).

[25]M. E. Cates, M. Fuchs, K. Kroy, W. C. K. Poon, and A. M. Puertas, "Theory and simulation of gelation, arrest and yielding in attracting colloids," J. Phys.: Condens. Matter **16**, S4861 (2004).

[26]C. J. Dibble, M. Kogan, and M. J. Solomon, "Structure and dynamics of colloidal depletion gels: Coincidence of transitions and heterogeneity," Phys. Rev. E. **74**, 041403 (2006).

[27]K. N. Pham, A. M. Puertas, J. Bergenholtz, S. U. Egelhaaf, A. Moussaïd, P. N. Pusey, A. B. Schofield, M. E. Cates, M. Fuchs, and W. C. K. Poon, "Multiple glassy states in a simple model system," Science **296**, 104–106 (2002).

[28]E. Zaccarelli, G. Foffi, K. A. Dawson, S. V. Buldyrev, F. Sciortino, and P. Tartaglia, "Confirmation of anomalous dynamical arrest in attractive colloids: A molecular dynamics study," Phys. Rev. E **66**, 041402 (2002).

[29]N. Simeonova, R. Dullens, D. Aarts, V. W. A. de Villeneuve, H. N. W. Lekkerkerker, and W. Kegel, "Devitrification of colloidal glasses in real space," Phys. Rev. E **73**, 041401 (2006).

[30]P. Charbonneau and D. R. Reichman, "Dynamical heterogeneity and nonlinear susceptibility in supercooled liquids with short-range attraction," Phys. Rev. Lett. **99**, 135701 (2007).

[31]Z. Zhang, P. J. Yunker, P. Habdas, and A. G. Yodh, "Cooperative rearrangement regions and dynamical heterogeneities in colloidal glasses with attractive versus repulsive interactions," Phys. Rev. Lett. **107**, 208303 (2011).

[32]C. K. Mishra, A. Rangarajan, and R. Ganapathy, "Two-step glass transition induced by attractive interactions in quasi-two-dimensional suspensions of ellipsoidal particles," Phys. Rev. Lett. **110**, 118301 (2013).

[33]A. M. Puertas, M. Fuchs, and M. E. Cates, "Dynamical heterogeneities close to a colloidal gel," J. Chem. Phys. **121**, 2813–2822 (2004).

[34]A. J. Archer and N. B. Wilding, "Phase behavior of a fluid with competing attractive and repulsive interactions," Phys. Rev. E **76**, 031501 (2007).

[35]H. Sedgwick, S. U. Egelhaaf, and W. C. K. Poon, "Clusters and gels in systems of sticky particles," J. Phys.: Condens. Matter **16**, S4913–S4922 (2004).

[36]C. L. Klix, C. P. Royall, and H. Tanaka, "Structural and dynamical features of multiple metastable glassy states in a colloidal system with competing interactions," Phys. Rev. Lett. **104**, 165702 (2010).

[37]S. Buzzaccaro, R. Rusconi, and R. Piazza, "'Sticky' hard spheres: Equation of state, phase diagram, and metastable gels," Phys. Rev. Lett. **99**, 098301 (2007).

[38]J. M. Olais-Gove, L. López-Flores, and M. Medina-Noyola, "Nonequilibrium theory of arrested spinodal decomposition," J. Chem. Phys. **143**, 174505 (2015).

[39]A. Ivlev, H. Löwen, G. E. Morfill, and C. P. Royall, *Complex Plasmas and Colloidal Dispersions: Particle-Resolved Studies of Classical Liquids and Solids* (World Scientific Publishing Co., Singapore Scientific, 2012).

[40]M. N. Bannerman, R. Sargant, and L. Lue, "Dynamo: A free O(n) general event-driven simulator," J. Comput. Chem. **32**, 3329–3338 (2011).

[41]J. Largo, M. A. Miller, and F. Sciortino, "The vanishing limit of the square-well fluid: The adhesive hard-sphere model as a reference system," J. Chem. Phys. **128**, 134513 (2008).

[42]C. P. Royall, A. A. Louis, and H. Tanaka, "Measuring colloidal interactions with confocal microscopy," J. Chem. Phys. **127**, 044507 (2007).

[43]M. Dijkstra, R. van Roij, and R. Evans, "Effective interactions, structure, and isothermal compressibility of colloidal suspensions," J. Chem. Phys. **113**, 4799–4807 (2000).

[44]C. P. Royall, W. C. K. Poon, and E. R. Weeks, "In search of colloidal hard spheres," Soft Matter **9**, 17–27 (2013).

[45]G. Bosma, C. Pathmamanoharan, E. H. A. de Hoog, W. K. Kegel, A. van Blaaderen, and H. N. W. Lekkerkerker, "Preparation of monodisperse, fluorescent pmma-latex colloids by dispersion polymerization," J. Colloid Interface Sci. **245**, 292–300 (2002).

[46]D. Zerrouki, B. Rotenberg, S. Abramson, J. Baudry, C. Goubault, F. Leal-Calderon, D. J. Pine, and J. Bibette, "Preparation of doublet, triangular, and tetrahedral colloidal clusters by controlled emulsification," Langmuir **22**, 57–62 (2006).

[47]S. Taylor, R. Evans, and C. P. Royall, "Temperature as an external field for colloid-polymer mixtures: 'Quenching' by heating and 'melting' by cooling," J. Phys.: Condens. Matter **24**, 464128 (2012).

[48]G. Foffi, C. D. Michele, F. Sciortino, and P. Tartaglia, "Scaling of dynamics with the range of interaction in short-range attractive colloids," Phys. Rev. Lett. **94**, 078301 (2005).

[49]A. Ninarello, L. Berthier, and D. Coslovich, "Models and algorithms for the next generation of glass transition studies," Phys. Rev. X **7**, 021039 (2017).

[50]W. C. K. Poon, F. Renth, R. Evans, D. Fairhurst, M. E. Cates, and P. N. Pusey, "Colloid-polymer mixtures at triple coexistence: Kinetic maps from free-energy landscapes," Phys. Rev. Lett. **83**, 1239–1242 (1999).

[51]K. G. Soga, J. R. Melrose, and R. C. Ball, "Metastable states and the kinetics of colloid phase separation," J. Chem. Phys. **110**, 2280–2288 (1999).

[52]F. Renth, W. C. K. Poon, and R. M. L. Evans, "Phase transition kinetics in colloid-polymer mixtures at triple coexistence: Kinetic maps from free-energy landscapes," Phys. Rev. E **64**, 031402 (2001).

[53]A. Fortini, E. Sanz, and M. Dijkstra, "Crystallization and gelation in colloidal systems with short-ranged attractive interactions," Phys. Rev. E **78**, 041402 (2008).

[54]C. P. Royall and A. Malins, "The role of quench rate in colloidal gels," Faraday Discuss. **158**, 301–311 (2012).

[55]J. Sabin, A. E. Bailey, G. Espinosa, and B. J. Frisken, "Crystal-arrested phase separation," Phys. Rev. Lett. **109**, 195701 (2012).

[56]T. H. Zhang, J. Klok, R. H. Tromp, J. Groenewold, and W. K. Kegel, "Non-equilibrium cluster states in colloids with competing interactions," Soft Matter **8**, 667–672 (2012).

[57]H. Tsurusawa, J. Russo, M. Leocmach, and H. Tanaka, "Formation of porous crystals via viscoelastic phase separation," Nat. Mater. **16**, 1022–1028 (2017).

[58]R. Rice, R. Roth, and C. P. Royall, "Polyhedral colloidal? rocks: Low-dimensional networks," Soft Matter **8**, 1163–1167 (2012).

[59]C. Royall, D. G. A. L. Aarts, and H. Tanaka, "Fluid structure in colloid-polymer mixtures: The competition between electrostatics and depletion," J. Phys.: Condens. Matter **17**, S3401–S3408 (2005).

[60]M. G. Noro and D. Frenkel, "Extended corresponding-states behavior for particles with variable range attractions," J. Chem. Phys. **113**, 2941–2944 (2000).

[61]A. A. Louis, P. G. Bolhuis, E. J. Meijer, and J. P. Hansen, "Polymer induced depletion potentials in polymer-colloid mixtures," J. Chem. Phys. **117**, 1893–1907 (2002).

[62]W. C. K. Poon, E. R. Weeks, and C. P. Royall, "On measuring colloidal volume fractions," Soft Matter **8**, 21–30 (2012).

[63]E. Zaccarelli, P. J. Lu, F. Ciulla, D. A. Weitz, and F. Sciortino, "Gelation as arrested phase separation in short-ranged attractive colloid-polymer mixtures," J. Phys.: Condens. Matter **20**, 494242 (2008).

[64]A. Malins, S. R. Williams, J. Eggers, and C. P. Royall, "Identification of structure in condensed matter with the topological cluster classification," J. Chem. Phys. **139**, 234506 (2013).

[65]C. P. Royall, S. R. Williams, T. Ohtsuka, and H. Tanaka, "Direct observation of a local structural mechanism for dynamic arrest," Nat. Mater. **7**, 556–561 (2008).

[66]J. Taffs, S. R. Williams, H. Tanaka, and C. P. Royall, "Structure and kinetics in the freezing of nearly hard spheres," Soft Matter **9**, 297–305 (2013).

[67] E. Sanz, C. Valeriani, W. C. K. Zaccarelli, E. Poon, P. N. Pusey, and M. E. Cates, "Crystallization mechanism of hard sphere glasses," Phys. Rev. Lett. **106**, 215701 (2011).

[68] M. Godogna, A. Malins, S. R. Williams, and C. P. Royall, "The local structure of the gas-liquid interfaces," Mol. Phys. **109**, 1393–1402 (2010).

[69] Comment made by Mark Miller: The method developed by Miller and Frenkel modeled the Baxter model, the limit of an infinitely thin, infinitely deep attractive well. Those authors focussed on the critical point and surrounding region. It is possible that the specialised technique they developed to successfully capture the limiting case of the Baxter model did not fully sample dense configurations leading to an underestimation of the liquid density, 2015.

[70] Y.-L. Chen and K. S. Schweizer, "Microscopic theory of gelation and elasticity in polymer-particle suspensions," J. Chem. Phys. **120**, 7212–7222 (2004).

[71] L. Berthier and W. Kob, "The Monte Carlo dynamics of a binary lennard-jones glass-forming mixture," J. Phys.: Condens. Matter **19**, 205130 (2007).

[72] A. Furukawa and H. Tanaka, "Key role of hydrodynamic interactions in colloidal gelation," Phys. Rev. Lett. **104**, 245702 (2010).

[73] C. P. Royall, J. Eggers, A. Furukawa, and H. Tanaka, "Probing colloidal gels at multiple length scales: The role of hydrodynamics," Phys. Rev. Lett. **114**, 258302 (2015).

[74] C. P. Royall and S. R. Williams, "C60: The first one-component gel?," J. Phys. Chem. B **115**, 7288–7293 (2011).

[75] G. Foffi, C. De Michele, F. Sciortino, and P. Tartaglia, "Arrested phase separation in a short-ranged attractive colloidal system: A numerical study," J. Chem. Phys. **122**, 224903 (2005).

[76] C. P. Royall and W. Kob, "Locally favoured structures and dynamic length scales in a simple glass-former," J. Stat. Mech.: Theory Exp. **2017**, 024001.

[77] V. Prasad, V. Trappe, A. D. Dinsmore, P. N. Segre, L. Cipelletti, and D. A. Weitz, "Universal features of the fluid to solid transition for attractive colloidal particles," Faraday Discuss. **123**, 1–12 (2003).

[78] H. Tanaka, J. Meunier, and D. Bonn, "Nonergodic states of charged colloidal suspensions: Repulsive and attractive glasses and gels," Phys. Rev. E **69**, 031404 (2004).

[79] D. Levis and L. Berthier, "Clustering and heterogeneous dynamics in a kinetic monte carlo model of self-propelled hard disks," Phys. Rev. E **89**, 062301 (2014).

[80] D. Fusco and P. Charbonneau, "Crystallization of asymmetric patchy models for globular proteins in solution," Phys. Rev. E **88**, 012721 (2013).

[81] E. Flenner, H. Staley, and G. Szamel, "Universal features of dynamic heterogeneity in supercooled liquids," Phys. Rev. Lett. **112**, 097801 (2014).

[82] A. Vrij, "Phase-transition phenomena in colloidal systems with attractive and repulsive particle interactions," Faraday Discuss. **90**, 31–40 (1990).

[83] S. Manley, H. M. Wyss, K. Miyazaki, J. C. Conrad, V. Trappe, L. J. Kaufman, D. R. Reichman, and D. A. Weitz, "Glasslike arrest in spinodal decomposition as a route to colloidal gelation," Phys. Rev. Lett. **95**, 238302 (2005).

[84] S. Griffiths, F. Turci, and C. P. Royall, "Local structure of percolating gels at very low volume fractions," J. Chem. Phys. **146**, 014905 (2017).